

# Size and shape control for water-soluble magnetic cobalt nanoparticles using polymer ligands

Le Trong Lu,<sup>a</sup> Le Duc Tung,<sup>b</sup> Ian Robinson,<sup>a</sup> Diane Ung,<sup>a</sup> Bien Tan,<sup>a</sup> James Long,<sup>c</sup> Andrew Ian Cooper,<sup>ae</sup> David Garth Fernig<sup>de</sup> and Nguyen Thi Kim Thanh<sup>\*ade</sup>

Received 31st January 2008, Accepted 11th March 2008

First published as an Advance Article on the web 1st April 2008

DOI: 10.1039/b801800f

We report a synthesis of monodisperse water-soluble magnetic Co nanoparticles using a facile reduction method in aqueous media in the presence of alkyl thioether end-functionalized poly(methacrylic acid) (PMAA-DDT) ligands. The size and shape of the nanoparticles are both tunable by varying synthesis conditions. The size of the spherical nanoparticles can be tuned between 2–7.5 nm by changing the concentration of the polymer. Our synthesis approach also provides a route for producing much larger spherical nanoparticles of 80 nm as well as anisotropic nanorods of 15 × 36 nm. The spherical nanoparticles are superparamagnetic at room temperature. The nanoparticles can be stable in water for up to eight weeks when 0.12 mM PMAA-DDT with molecular weight of 13500 g mol<sup>-1</sup> is used as ligand.

## Introduction

Recently there has been a great deal of interest in the applications of magnetic nanoparticles (NPs) in biomedicine including magnetic separation, cell labeling, targeted drug delivery, hyperthermia treatment of solid tumors, and magnetic resonance imaging (MRI).<sup>1–6</sup> In these applications, the NPs must be water-soluble, chemically stable, biocompatible, superparamagnetic at room temperature (to avoid aggregation), capable of recognizing the biological targets,<sup>7</sup> and size comparable to bio-molecules.<sup>8</sup> In many cases, it is also desirable that the magnetic NPs have large magnetization and high magnetic susceptibility so that they can respond sensitively to a small external magnetic field or the signal of a magnetic sensor. Hence, the choice of materials and the particle size are very important. Magnetic transition metals such as Co and Fe have saturation magnetizations more than twice those of iron oxides (*i.e.* Fe<sub>2</sub>O<sub>3</sub> and Fe<sub>3</sub>O<sub>4</sub>).<sup>9</sup> However, these metals are very susceptible to oxidation, making the NPs unstable and causing loss in response to the external magnetic field. To avoid oxidation, NPs have been coated with an additional inorganic layer such as silica,<sup>10,11</sup> but this extra step is somewhat cumbersome and also increases the mass of the NPs. The size of the magnetic NPs has two opposing effects. Larger size gives rise to higher magnetization in the particles, but also causes an increase in particle mass which then necessitates a higher external magnetic field for some applications. Thus, for a particular application, an optimal particle size is required; as

such, the ability to synthesize NPs with fine size control is very important.

A limited number of water-soluble magnetic nanomaterials exist including Fe<sub>2</sub>O<sub>3</sub>,<sup>12–16</sup> Fe<sub>3</sub>O<sub>4</sub>,<sup>17–22</sup> CoPt<sub>3</sub><sup>16</sup> and Co.<sup>10,11,23,24</sup> Different sizes of NPs can be achieved by varying the synthesis conditions in organic solvents.<sup>25–28</sup> However, to date, there has been no report of tuning the particle size of the magnetic materials using water as the synthetic medium. In the case of water-soluble Co NPs, most syntheses have been carried out directly in water in the presence of ligands such as peptides,<sup>7</sup> citrate,<sup>10,11</sup> glycolipids,<sup>23</sup> or other templates.<sup>24</sup> However, these Co NPs are rather polydisperse,<sup>23,24</sup> and unstable.<sup>7</sup> Recently, taking advantage of the properties of thermo-responsive polymers, we have reported the synthesis of monodisperse Co NPs in an organic solvent at high temperatures.<sup>29</sup> The as-prepared Co NPs were water soluble below 25 °C due to the conformational change of the polymer from hydrophobic (at high temperature) to hydrophilic (at lower temperature). This novel approach is useful for making water-soluble Co NPs, however, the size of the NPs is still relatively uncontrolled.

In this paper, we report a facile synthesis of monodisperse water-soluble Co NPs in which both size *and* shape can be controlled. The as-prepared NPs were found to be stable in water at room temperature for as long as eight weeks. Here, our strategy in the synthesis is based on the use of alkyl thioether end-functionalized poly(methacrylic acid) (PMAA-DDT) ligands, as recently exploited in the synthesis of size-controlled water-soluble Au NPs.<sup>30,31</sup> Moreover, the carboxylic groups of the coating PMAA-DDT polymer can be conjugated with amines in the biomolecules, thus our synthesized Co NPs could be exploited for many potential biomedical applications. Our recent investigations have indicated that the as-prepared Co NPs could be used as the contrast agent in MRI, in which the signal is significantly improved compared with conventional iron oxides.<sup>32</sup> Co<sup>2+</sup> is necessary for health in small quantities (0.01 mg day<sup>-1</sup>), but higher doses (≥10 mg day<sup>-1</sup>) may result in

<sup>a</sup>Department of Chemistry, University of Liverpool, Crown Street, UK L69 7ZD. E-mail: ntktanh@liv.ac.uk

<sup>b</sup>Department of Physics, University of Liverpool, Crown Street, UK L69 3BX

<sup>c</sup>Iota NanoSolutions Ltd, Crown Street, Liverpool, UK L69 7ZB

<sup>d</sup>School of Biological Sciences, University of Liverpool, Crown Street, UK L69 7ZB

<sup>e</sup>Liverpool Institute for Nanoscale Science Engineering and Technology (LINSET), University of Liverpool, Crown Street, UK L69 7ZB

cardiomyopathy.<sup>33</sup> The potential toxicity of Co in the form of a passivated metal has yet to be established and there are currently no data on the toxicity of the Co NPs. Stable Co NPs will present their ligand shell to the body and may not have any metal-associated toxicity.

## Experimental

### Materials

All materials were used without further purification. Cobalt(II) chloride (97%) and sodium borohydride (98%) were purchased from Aldrich Ltd, UK and Fisher Ltd, UK, respectively. Alkyl thioether end-functionalized poly(methacrylic acid) (PMAA-DDT) with different molecular weights ( $M_w$ ) (2 500, 2 750, 3 420, 3 640, 7 000, 8 610 and 13 500 g mol<sup>-1</sup>) and poly(methacrylic acid) (PMAA) with molecular weight of 13 000 g mol<sup>-1</sup> were synthesized as described previously.<sup>30,31</sup>

### Synthesis of Co nanoparticles

Co NPs were prepared by reduction of Co<sup>2+</sup> in water in the presence of the polymer ligand. In a typical procedure, the reductant, NaBH<sub>4</sub>, and the polymer were added to a 250 ml two-necked flask which was then de-gassed by purging with N<sub>2</sub> for 30 min. To this flask, degassed and de-ionised water (49 ml) was added and the mixture was sonicated for 7–12 min in a U300 Ultrawave sonic bath (Ultrawave Ltd, UK) to dissolve the polymer and the reductant. CoCl<sub>2</sub> solution was freshly prepared by dissolving 65 mg (0.5 mmol) of CoCl<sub>2</sub> in degassed water (1 ml). This solution was rapidly injected into the reaction flask under sonication. The final concentrations of NaBH<sub>4</sub> and CoCl<sub>2</sub> in the reaction flask were 100 mM and 10 mM, respectively. Sonication was continued for 3 min after the injection. During this time, the solution changed rapidly to a dark near-black color with significant gas evolution. After 1 h, five 1 ml fractions were withdrawn and stored in small glass vials for morphology determination using transmission electron microscopy (TEM) and visual observation of the stability of the NPs.

### Characterization

The morphology and size of the NPs were determined using a FEI Tecnai G<sup>2</sup> 120 kV TEM, operated at 100 kV and visualized using analySIS software. The diameter ( $d$ ) of the NPs and their size distribution were taken as the mean of minimum 200 NPs measured from enlarged photographs using Bersoft Image Measurement 1.0 software. The  $\zeta$ -potential measurements were taken from a Zetasizer Nano S (Zen 3600), Malvern Instruments Ltd, UK. Magnetic measurements, including the zero-field-cooled and field-cooled magnetization, were carried out in a Quantum Design MPMS SQUID magnetometer.

## Results and discussion

### Effect of the synthesis conditions on the morphology of the synthesized Co NPs

The direct reduction of Co<sup>2+</sup> in water in the presence of PMAA-DDT polymer produced Co NPs. We studied the effect of the synthesis conditions on the morphology of the NPs. First, the

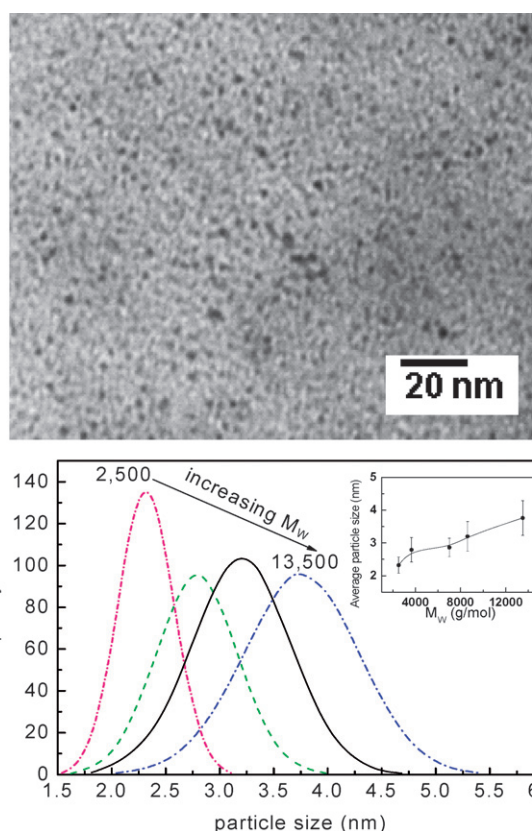


**Fig. 1** TEM image of the Co NPs synthesized in the presence of the PMAA-DDT polymer (molecular weight  $M_w = 8610$  g mol<sup>-1</sup>) (upper panel); size distribution histograms of the Co NPs synthesized in the presence of PMAA-DDT polymers with different molecular weights at a concentration of 0.12 mM (bottom panel); the inset shows the average particle size as a function of the polymer molecular weight.

polymer concentration was fixed at 0.12 mM, and the polymer molecular weight varied from 2 500 to 13 500 g mol<sup>-1</sup>. Fig. 1 shows a TEM image of the Co NPs synthesized with the polymer ligand at  $M_w = 8610$  g mol<sup>-1</sup> as an example. The size distribution histograms and the average particle size for different Co NPs are also included in Fig. 1. Small, monodisperse particles in a narrow size range of  $2.3 \pm 0.2$  nm to  $3.8 \pm 0.5$  nm were obtained and it was found that the average particle size increased with increasing polymer molecular weight. Previously, a similar relationship between the average particle size and the PMAA-DDT polymer molecular weight was also found for Au NPs and this was attributed to the heteroatom-containing polymer acting as a “net” to assist particle nucleation.<sup>34</sup> In the case of Co, we believe that the higher molecular weight polymers may both supply metal atoms more efficiently in this manner and also lead to a slower rate of diffusion and greater passivation of the growing clusters, thus resulting in larger NPs.

In order to extend the range of obtainable particle size, we focused on the PMAA-DDT polymer with  $M_w = 13500$  g mol<sup>-1</sup>, which produced the largest Co NPs (average diameter 3.8 nm; Fig. 1). By varying the polymer concentration, we found that it was also possible to control the size of the Co NPs. Fig. 2 shows a TEM image of the Co NPs in which the synthesis was carried out at a polymer concentration of 0.12 mM. The size distribution

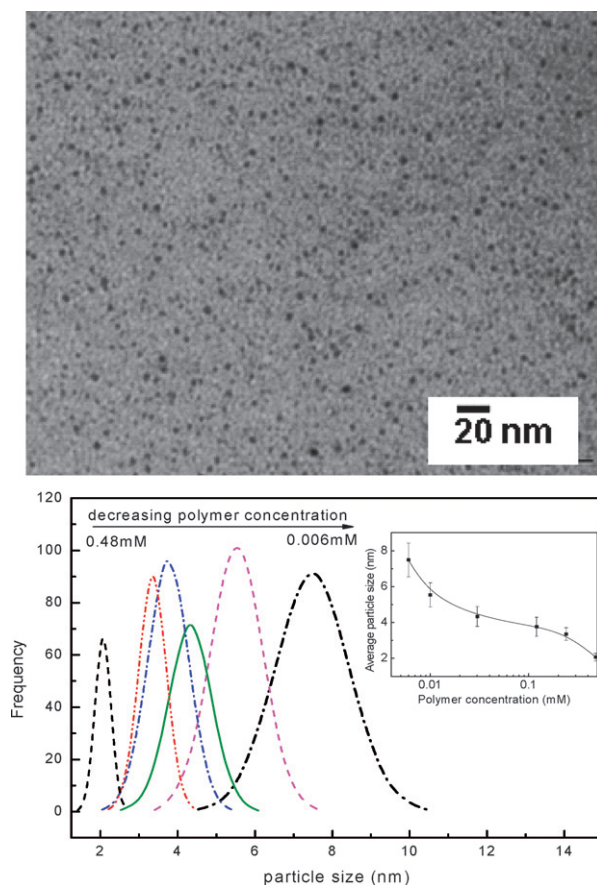


**Fig. 2** TEM image of the Co NPs synthesized in the presence of the PMAA-DDT polymer at a concentration of 0.12 mM (upper panel); size distribution histograms of the Co NPs at different polymer concentrations (bottom panel); the inset shows the average particle size as a function of the polymer concentration. The polymer molecular weight was  $13\,500\text{ g mol}^{-1}$ .

histograms of the Co NPs synthesized with the same polymer, but at different polymer concentrations, are also included in Fig. 2. It can be seen that the average particle size increases with decreasing polymer concentration. With the polymer concentration in the range of 0.006 mM to 0.48 mM, the average particle size can be tuned between  $7.5 \pm 0.7$  and  $2.1 \pm 0.2$  nm. The fact that the size of the Co NPs could be tuned over a broader range by varying the polymer concentration rather than the polymer molecular weight is comparable with results obtained for Au NPs prepared using these polymer ligands.<sup>31</sup>

When the polymer concentration was diluted further (0.0048 mM), uniform rod-like particles with an average length of 36 nm and an average width of 15 nm were obtained (Fig. 3). This transition was found to be repeatable at this concentration of the polymer. Previously, Co nanorods were synthesized in organic solvent using non-commercially available organometallic complex  $[\text{Co}(\eta^3\text{-C}_8\text{H}_7)(\eta^4\text{-C}_8\text{H}_7)]$ .<sup>35</sup> In contrast, here Co nanorods were obtained from a simple reduction of inexpensive  $\text{CoCl}_2$ . To the best of our knowledge, this is the first example of cobalt nanorods synthesized in aqueous media.

In spite of extensive studies on the formation of Au nanorods, the mechanism of their formation in aqueous media remains unclear.<sup>36</sup> In case of the Co NPs, one possibility is that the  $\text{Co}^{2+}$

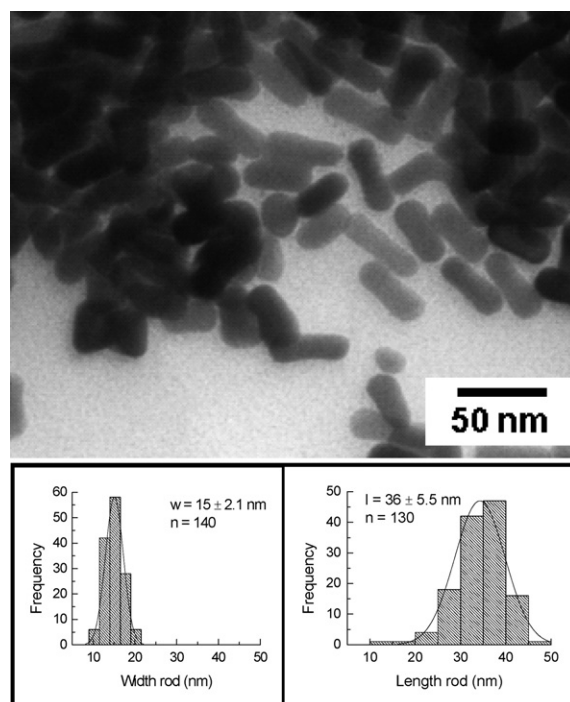


**Fig. 3** TEM image and the corresponding histograms of  $36 \times 15$  nm Co nanorods synthesized in the presence of the PMAA-DDT polymer at a molecular weight  $M_W = 13\,500\text{ g mol}^{-1}$  and a concentration of 0.0048 mM.

cations complex with carboxylate anions in the polymer ligand. Thus, when the polymer concentration is below a certain threshold, this causes the preferential growth at specific crystallographic facets of the NPs, due to preferential adsorption of the polymer–cobalt complex to particular crystal facets during the growth of the NPs.

To further increase the particle size, the effect on the particle morphology by changing the order of addition between the reductant ( $\text{NaBH}_4$  solution) and the  $\text{CoCl}_2$  precursor solution was investigated using the polymer with  $M_W = 13\,500\text{ g mol}^{-1}$ . We kept the same concentration of all starting materials constant, but the reductant  $\text{NaBH}_4$  solution was introduced after first dissolving both the  $\text{CoCl}_2$  precursor and the polymer together in water. In this case, it was found that the speed of adding the reductant has a profound effect on the nucleation and growth processes for the Co NPs, resulting in very different average particle sizes. When the reductant was rapidly injected, large Co NPs of about 81 nm were obtained in comparison with  $4.4 \pm 0.6$  nm when the reductant was introduced drop-wise (see Fig. 4).

The magnetic properties of the Co NPs, including the zero-field-cooled (ZFC) and field-cooled (FC) magnetization, were investigated and results are presented in Fig. 5. The splitting between the ZFC and FC curves occurs fairly close to the peak observed in the ZFC curve, suggesting that the samples are quite uniform and monodisperse to be in agreement with the TEM results. From the peak of the ZFC curve, the blocking temperature can be determined and its values as a function of the average particle size are also plotted (Fig. 5). With an average particle size of 7.5 nm, the Co NPs have a blocking temperature  $T_B$

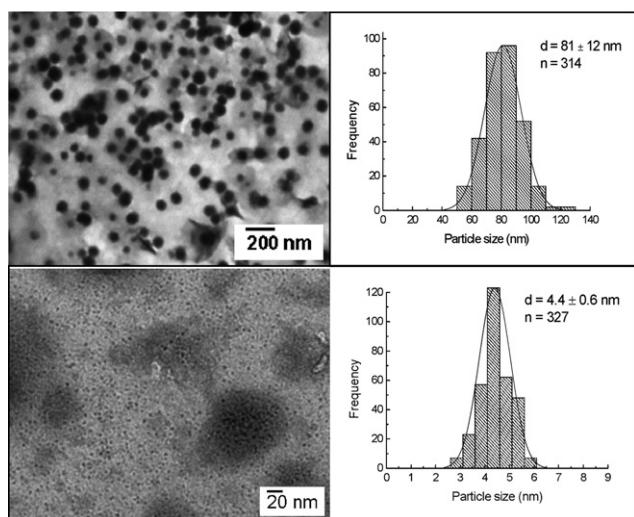


**Fig. 4** TEM images and the corresponding size distribution histograms of the Co NPs synthesized by rapid injection (top panels) or drop-wise addition (bottom panels) of the reductant  $\text{NaBH}_4$  into the mixture of  $\text{CoCl}_2$  solution and the polymer. The polymer molecular weight was  $13\,500\text{ g mol}^{-1}$  and the polymer concentration was  $0.12\text{ mM}$ .

of about  $283\text{ K}$  and this decreases with decreasing average particle size.

#### Stability of the NPs

The polymer ligand, PMAA, is a weak polyelectrolyte and can provide both steric and electrostatic repulsion between the NPs to prevent them from aggregating.<sup>34</sup> On the other hand, since the standard reduction potential of  $\text{Co}^{2+}/\text{Co}$  is low ( $-0.28\text{ V}$ ), it is very susceptible to oxidation, especially at the nanoscale. The formation of an oxidized cobalt layer might disrupt the coordinative bonding between the Co core and the coating polymer layer, which could then compromise the stabilizing repulsion between the NPs.

We have observed that, over long time periods, the as-prepared NPs become aggregated and precipitated from the aqueous solution and thus the stability time for these aqueous solutions could be monitored visually. There also appeared to be a chemical reaction taking place inside the sediments on a longer timescale forming complexes containing  $\text{Co}^{2+}$  ions and this gave rise to a pale green color in the solution (see Fig. 6, inset).

Fig. 6 shows the stability time for aqueous solutions containing the Co NPs coated with PMAA-DDT with different molecular weights and at two polymer concentrations of  $0.06$  and  $0.12\text{ mM}$ . It can be seen that the stability is enhanced at a polymer concentration of  $0.12\text{ mM}$ . A further increase in the polymer concentration beyond  $0.12\text{ mM}$ , however, did not improve the stability time for the NPs (data not shown). Increasing the polymer molecular weight also tends to improve the stability time of the NPs quite markedly at a given concentration. The greatest stability was observed with a polymer molecular weight of  $13\,500\text{ g mol}^{-1}$ , and the Co NPs remained well dispersed in aqueous solution for up to eight weeks after the synthesis. As mentioned above, we observed that the particle size increased with the polymer molecular weight. It is, therefore, likely that the smaller NPs are more susceptible to oxidation. It is also possible

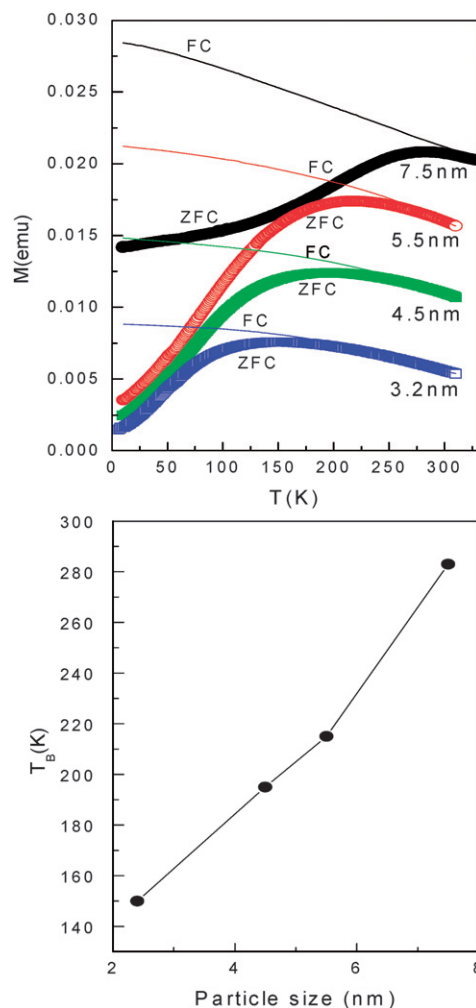


**Fig. 5** The zero-field-cooled (ZFC) and field-cooled (FC) magnetization of the as-prepared Co NPs with different sizes (upper panel) and the blocking temperature  $T_B$  as a function of the average particle size (bottom panel).

that, as a result of increasing the polymer molecular weight, a thicker/denser polymer layer forms which then better protects the Co core from oxidation as well as increasing the steric and electrostatic repulsion between the NPs.

The thioether DDT end-group was also found to play an important role in determining the stability of the NPs. The NPs coated only with PMAA ( $M_W = 13\,000\text{ g mol}^{-1}$ , no thioether end-group) began to precipitate from the aqueous solution after just 11 days. This may be attributed to a strong adsorption of the hydrophobic DDT onto the surfaces of the NPs, which would enhance the attachment of the polymer ligand to the Co core and hence increase the stability time of the NPs.

We have also investigated the  $\zeta$ -potential, which is a measure of the surface charge on the NPs in different aqueous solutions. A large (absolute) value of the  $\zeta$ -potential indicates the high surface charge, strong particle repulsion, and high stability of the NPs in solution. At a fixed pH, the exposure of charged domains increases as the molecular weight of the coating polymer layer increases, resulting in an increase of the absolute value of the  $\zeta$ -potential (see, for example, Fig. 7a).

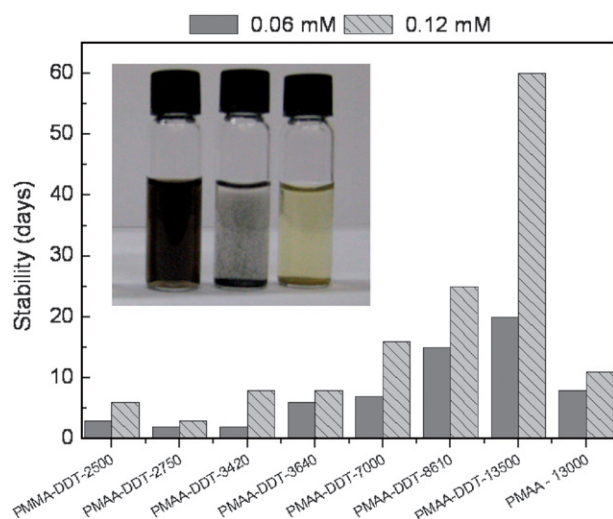


**Fig. 6** Stability time for the Co NPs synthesized with different polymers at concentrations of 0.06 and 0.12 mM. The inset shows a picture of the solutions containing stable water-soluble Co NPs (left), the deteriorated (not stable) Co NPs (middle), and complexes containing  $\text{Co}^{2+}$  ions (right).

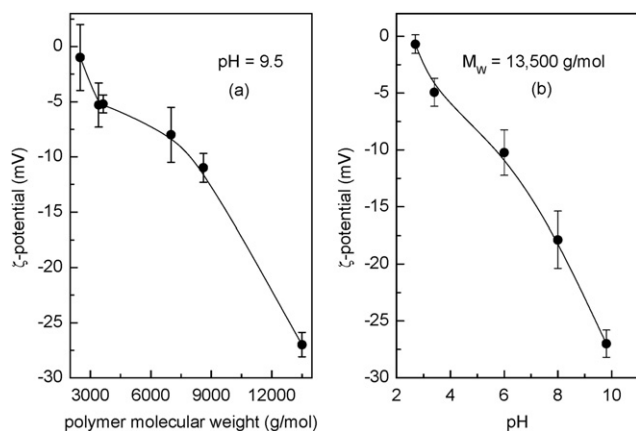


**Fig. 7** The  $\zeta$ -potential as a function of the PMAA-DDT polymer molecular weight (left panel) and of pH (right panel).

Similarly, when the molecular weight of the coating polymer layer is fixed, we observed that increasing pH also results in an increase of the absolute value of the  $\zeta$ -potential (Fig. 7b). In this case, the dependence of the  $\zeta$ -potential upon pH could be attributed to an increase in the particle surface ionization of which a contribution is most likely due to deprotonation of the carboxylic acid groups in the polymer ligand chains under increasingly basic conditions.

## Conclusion

Our one-step synthetic approach to produce controlled size and shape monodisperse water-soluble Co NPs is simple and novel. The reduction of  $\text{CoCl}_2$  in aqueous media produces the Co NPs that are readily water soluble and can be used directly for biomedical assays such as a MRI contrast enhancer.<sup>32</sup> In addition, the PMAA-DDT polymer coating can be conjugated directly with biomolecules *via* the carboxylic groups, our synthesised Co NPs could be potentially exploited further for

other biomedical applications (*e.g.*, magnetic separation, immunoassays, stem cell tracking, cancer metastasis monitoring using MRI, targeted drug delivery, and hyperthermia cancer treatment), though the pharmacokinetics and toxicology of these materials remain to be established. The formation of the Co nanorods in water will open up new routes for many interesting studies where the physical properties (magnetic response, MR relaxivities, dipole–dipole interactions) of the NPs depend on their anisotropic shapes. It is also interesting to see the effect of cellular uptake on the different shaped NPs. The formation of well ordered monolayer films of Co nanorods can be conducted in a similar way to Co NPs.<sup>37</sup>

## Acknowledgements

This work was supported by the Royal Society, Vietnamese Government (322 project), the North West Cancer Research Fund, the Engineering and Physical Sciences Research Council (EP/C511794/1) and the Wellcome Trust. The authors thank Dr Ian Prior for provision of the TEM facilities.

## References

- 1 Q. A. Pankhurst, J. Connolly, S. K. Jones and J. Dobson, *J. Phys. D: Appl. Phys.*, 2003, **36**, R167–R181.
- 2 A. K. Gupta and M. Gupta, *Biomaterials*, 2005, **26**, 3995–4021.
- 3 C. C. Berry and A. S. G. Curtis, *J. Phys. D: Appl. Phys.*, 2003, **36**, R198–R206.
- 4 S. Mornet, S. Vasseur, F. Grasset, P. Veverka, G. Goglio, A. Demourgues, J. Portier, E. Pollert and E. Duguet, *Prog. Solid State Chem.*, 2006, **34**, 237–247.
- 5 T. Neuberger, B. Schopf, H. Hofmann, M. Hofmann and B. von Rechenberg, *J. Magn. Magn. Mater.*, 2005, **293**, 483–496.
- 6 N. T. K. Thanh, I. Robinson and L. D. Tung, in *Dekker Encyclopedia of Nanoscience and Nanotechnology*, ed. J. A. Schwarz, C. C. Oates and K. Putyera, Taylor and Francis Group, LLC, New York, 2007, vol. 1, pp. 1–10.
- 7 N. T. K. Thanh, V. F. Puentes, L. D. Tung and D. G. Fernig, *J. Phys.: Conf. Ser.*, 2005, **17**, 70–76.
- 8 S. Mornet, S. Vasseur, F. Grasset and E. Duguet, *J. Mater. Chem.*, 2004, **14**, 2161–2175.
- 9 *Magnetic oxides*, ed. D. J. Clark, Wiley, New York, 1972.
- 10 V. Salgueirino-Maceira, M. A. Correa-Duarte, M. Farle, M. A. Lopez-Quintela, K. Sieradzki and R. Diaz, *Langmuir*, 2006, **22**, 1455–1458.
- 11 M. Aslam, S. Li and V. P. Dravid, *J. Am. Ceram. Soc.*, 2007, **90**, 950–956.
- 12 S. J. Lee, J. R. Jeong, S. C. Shin, Y. M. Huh, H. T. Song, J. S. Suh, Y. H. Chang, B. S. Jeon and J. D. Kim, *J. Appl. Phys.*, 2005, **97**, 10Q913.
- 13 S. Yu and G. M. Chow, *J. Mater. Chem.*, 2004, **14**, 2781–2786.
- 14 L. E. Euliss, S. G. Grancharov, S. O'Brien, T. J. Deming, G. D. Stucky, C. B. Murray and G. A. Held, *Nano Lett.*, 2003, **3**, 1489–1493.
- 15 Y. Wang, J. F. Wong, X. W. Teng, X. Z. Lin and H. Yang, *Nano Lett.*, 2003, **3**, 1555–1559.
- 16 T. Pellegrino, L. Manna, S. Kudera, T. Liedl, D. Koktysh, A. L. Rogach, S. Keller, J. Radler, G. Natile and W. J. Parak, *Nano Lett.*, 2004, **4**, 703–707.
- 17 Y. S. Kang, S. Risbud, J. F. Rabolt and P. Stroeve, *Chem. Mater.*, 1996, **8**, 2209–2211.
- 18 H. B. Xia, J. B. Yi, P. S. Foo and B. H. Liu, *Chem. Mater.*, 2007, **19**, 4087–4091.
- 19 L. A. Harris, J. D. Goff, A. Y. Carmichael, J. S. Riffle, J. J. Harburn, T. G. St Pierre and M. Saunders, *Chem. Mater.*, 2003, **15**, 1367–1377.
- 20 J. J. Yuan, S. P. Armes, Y. Takabayashi, K. Prassides, C. A. P. Leite, F. Galembeck and A. L. Lewis, *Langmuir*, 2006, **22**, 10989–10993.
- 21 W. W. Yu, E. Chang, C. M. Sayes, R. Drezek and V. L. Colvin, *Nanotechnology*, 2006, **17**, 4483–4487.

- 
- 22 M. Kim, Y. F. Chen, Y. C. Liu and X. G. Peng, *Adv. Mater.*, 2005, **17**, 1429–1432.
- 23 M. Kasture, S. Singh, P. Patel, P. A. Joy, A. A. Prabhune, C. V. Ramana and B. L. V. Prasad, *Langmuir*, 2007, **23**, 11409–11412.
- 24 N. Galvez, P. Sanchez, J. M. Dominguez-Vera, A. Soriano-Portillo, M. Clemente-Leon and E. Coronado, *J. Mater. Chem.*, 2006, **16**, 2757–2761.
- 25 T. Hyeon, S. S. Lee, J. Park, Y. Chung and H. B. Na, *J. Am. Chem. Soc.*, 2001, **123**, 12798–12801.
- 26 J. Park, K. J. An, Y. S. Hwang, J. G. Park, H. J. Noh, J. Y. Kim, J. H. Park, N. M. Hwang and T. Hyeon, *Nat. Mater.*, 2004, **3**, 891–895.
- 27 S. H. Sun and C. B. Murray, *J. Appl. Phys.*, 1999, **85**, 4325–4330.
- 28 N. S. Sobal, M. Hilgendorff, H. Mohwald, M. Giersig, M. Spasova, T. Radetic and M. Farle, *Nano Lett.*, 2002, **2**, 621–624.
- 29 I. Robinson, C. Alexander, L. T. Lu, L. D. Tung, D. G. Fernig and N. T. K. Thanh, *Chem. Commun.*, 2007, 4602–4604.
- 30 I. Hussain, S. Graham, Z. X. Wang, B. Tan, D. C. Sherrington, S. P. Rannard, A. I. Cooper and M. Brust, *J. Am. Chem. Soc.*, 2005, **127**, 16398–16399.
- 31 Z. X. Wang, B. E. Tan, I. Hussain, N. Schaeffer, M. F. Wyatt, M. Brust and A. I. Cooper, *Langmuir*, 2007, **23**, 885–895.
- 32 M. P. Laura, H. Richard, L. T. Lu, R. Ian, D. G. Fernig and N. T. K. Thanh, *Contrast Media Mol. Imaging*, 2008, submitted.
- 33 C. Alexander, *Am. J. Med.*, 1972, **53**, 395–417.
- 34 R. G. Shimmin, A. B. Schoch and P. V. Braun, *Langmuir*, 2004, **20**, 5613–5620.
- 35 F. Dumestre, B. Chaudret, C. Amiens, M. Respaud, P. Fejes, P. Renaud and P. Zurcher, *Angew. Chem., Int. Ed.*, 2003, **42**, 5213–5216.
- 36 J. Perez-Juste, I. Pastoriza-Santos, L. M. Liz-Marzan and P. Mulvaney, *Coord. Chem. Rev.*, 2005, **249**, 1870–1901.
- 37 M. Giersig and M. Hilgendorff, *J. Phys. D: Appl. Phys.*, 1999, **32**, L111–L113.